First-principles investigation of the relation between structural and NMR parameters in vitreous GeO_2

2010 J. Phys.: Condens. Matter 22 145501

(http://iopscience.iop.org/0953-8984/22/14/145501)

J. Phys.: Condens. Matter **22** (2010) 145501 (5pp) doi:10.1088/0953-8984/22/14/145501

First-principles investigation of the relation between structural and NMR parameters in vitreous GeO_2

Mikhail Kibalchenko[1], **Jonathan R Yates**[2] **and Alfredo Pasquarello**[3,4]

[1] TCM Group, Cavendish Laboratory, University of Cambridge, Cambridge CB3 0HE, UK
[2] Department of Materials, University of Oxford, Oxford OX1 3PH, UK
[3] Institute of Theoretical Physics, Ecole Polytechnique Fédérale de Lausanne (EPFL), CH-1015 Lausanne, Switzerland
[4] Institut Romand de Recherche Numérique en Physique des Matériaux (IRRMA), CH-1015 Lausanne, Switzerland

E-mail: mk531@cam.ac.uk

Received 26 January 2010, in final form 15 February 2010
Published 19 March 2010
Online at stacks.iop.org/JPhysCM/22/145501

Abstract
NMR parameters of ^{73}Ge and ^{17}O in vitreous GeO_2 and quartz GeO_2, including the isotropic shifts, the quadrupole coupling constants C_Q, and the electric-field-gradient asymmetry parameters η, are determined through density functional calculations. Clear correlations are established between ^{73}Ge shifts and the mean of the four neighboring Ge–O–Ge bond angles, and between C_Q and η parameters of ^{17}O and the local Ge–O–Ge angle. Available experimental data for C_Q and the corresponding established correlation are used to extract the value of 135° for the average Ge–O–Ge angle in vitreous GeO_2. The features of the Ge–O–Ge bond angle distribution of vitreous GeO_2 derived in this work are consistent with those inferred from other experimental probes.

(Some figures in this article are in colour only in the electronic version)

1. Introduction

The structures of glasses such as vitreous GeO_2 have been subject to thorough experimental and theoretical studies, especially for optical applications [1]. In comparison with other glasses such as SiO_2, vitreous GeO_2 possesses several advantageous properties including high refractive index, high transmittance over a wide spectral range, and minimal optical losses at wavelengths longer than IR [2, 3]. More recently, GeO_2 has reappeared on the scene in microelectronic research, as the native oxide of germanium, in the search for high-mobility materials alternative to silicon [4].

The short-range order in vitreous GeO_2 is well characterized by diffraction probes [5–8], and is determined by a tetrahedral structural unit, as in the crystalline structure of quartz GeO_2. The tetrahedra consist of Ge atoms at the center of four O atoms and form a continuous random network through connections at their corners. The disorder sets in on medium-range length scales and is described by the distribution of the Ge–O–Ge bond angles. The most recent neutron diffraction study places the average Ge–O–Ge bond angle at 132° [7, 8], in agreement with previous determinations [5]. However, access to the medium-range order is notoriously difficult for diffraction probes, because of overlapping correlations.

In recent years, significant attention has been devoted to the interpretation of experimental data obtained through alternative probes which could indirectly provide information about the underlying medium-range structure. Such developments are made possible by the high accuracy attained by simulation techniques based on density functional theory, which contribute to establishing a link between the measured property and the underlying structure. In this spirit, recent theoretical work on oxide networks has shown that Raman spectra are particularly sensitive to medium-range correlations [9–13]. In particular, for vitreous GeO_2, the

experimental Raman spectra were found to be consistent with an average Ge–O–Ge bond angle of ∼135° [11], in good agreement with the neutron diffraction data.

Solid-state nuclear magnetic resonance (NMR) is another experimental technique that has proved to be sensitive to medium-range correlations in both crystalline and non-crystalline materials, often providing information that is complementary to x-ray and neutron diffraction experiments. First-principles quantum mechanical calculations can provide the link between experimental NMR parameters and the underlying atomic structure. Such an approach has successfully been applied to a variety of systems, including zeolite ferrierites [14], silica [15], boron oxide [13], calcium aluminosilicate [16], and sodium tetrasilicate [17].

In this work, we study the NMR parameters of vitreous GeO_2 within a density functional scheme. Using atomistic model structures of vitreous GeO_2, we investigate correlations between these parameters and the underlying structural properties. In particular, we focus on establishing correlations between the NMR parameters and the local Ge–O–Ge bond angles.

2. Computational details

As model structures of vitreous GeO_2, we adopted models which were previously generated through classical and first-principles simulation methods in [10, 11]. These models consist of a defect-free network of cornersharing tetrahedra and were validated through comparisons with experiment for diffraction structure factors and vibrational spectra [10, 11]. We used model I and IV, which contain 168 and 36 atoms, respectively, which we refer to as model A and model B in the following. The distribution of Ge–O bond lengths in model A (B) shows an average value of 1.780 Å (1.771 Å) and a standard deviation of 0.014 Å (0.011 Å). The average bond lengths thus agree with the experimental value within a few per cent [10, 11]. In accord with experimental observations, the basic tetrahedral unit is well preserved with a mean O–Ge–O angle 109.4° for both models and with rms values of 5.8° for model A and 6.4° for model B. The medium-range order is described by the Ge–O–Ge bond angle distribution, which shows an average value of 135.0° for model A and 130.2° for model B. The standard deviations of these distributions are similar for the two models, with values of 10.6° and 10.9°, respectively. Both models have the experimental density of ∼3.65 g cm^{-3}. To provide a suitable reference for the NMR calculation, we also considered the quartz GeO_2 structure as determined by neutron diffraction at room temperature [18, 19].

Magnetic shielding and electric field gradient (EFG) tensors were calculated for both GeO_2 models using the gauge including projector augmented wave (GIPAW) [20] approach implemented in the CASTEP code [21, 22]. This approach uses periodic boundary conditions, which make our systems infinite. The CASTEP code uses a plane-wave basis implementation of density functional theory (DFT). All calculations were carried out using ultrasoft pseudopotentials [23] with the PBE (Perdew–Burke–Ernzerhof) [24] exchange–correlation functional and a maximum plane-wave energy of 500 eV. In the construction of pseudopotentials, oxygen 2s and 2p electrons were treated as valence. Core radii cut-offs were set to 1.0 au, 1.3 au, and 0.7 au for local, non-local and augmentation charges respectively. Germanium 3d, 4s, and 4p electrons were treated as valence. Core radii cut-offs were set to 2.0 au, 2.0 au, and 1.5 au for local, non-local and augmentation charges respectively. The non-local pseudopotential projectors were also used for the GIPAW reconstruction. The Brillouin zone was sampled using a Monkhorst–Pack [25] grid with a maximum spacing of 0.055 Å^{-1}. These parameters were chosen to converge the results to within 2 ppm for ^{73}Ge and ^{17}O shieldings and within 0.1 MHz for ^{73}Ge and ^{17}O quadrupole coupling constants.

Isotropic shieldings, $\sigma_{\rm iso}$, were calculated for each atom in the models using

$$\sigma_{\rm iso} = \tfrac{1}{3}(\sigma_{11} + \sigma_{22} + \sigma_{33}), \tag{1}$$

where σ_{ii} are the principal components of the symmetric part of the magnetic shielding tensor. Experiment provides the isotropic chemical shift $\delta_{\rm iso}$ which is defined relative to a reference shielding $\sigma_{\rm ref}$ such that

$$\delta_{\rm iso} = -(\sigma_{\rm iso} - \sigma_{\rm ref}). \tag{2}$$

We used $\sigma_{\rm ref} = 1215$ ppm for ^{73}Ge and $\sigma_{\rm ref} = 243$ ppm for ^{17}O. These reference values are worked out by imposing a constraint that the calculated shieldings for quartz GeO_2 fit the experimental ^{73}Ge result of $\delta_{\rm iso} = -110$ ppm [26] and the experimental ^{17}O result of $\delta_{\rm iso} = 49.5$ ppm [27]. However, a lack of experimental ^{73}Ge NMR results means that we cannot check our $\sigma_{\rm ref} = 1215$ ppm against other experiments. Quadrupole coupling constants $C_{\rm Q}$ and asymmetry parameters η were calculated from the EFG tensor [28, 14],

$$C_{\rm Q} = \frac{eQV_{zz}}{h} \tag{3}$$

$$\eta = \frac{V_{xx} - V_{yy}}{V_{zz}} \tag{4}$$

where V_{xx}, V_{yy}, and V_{zz} are the eigenvalues of the EFG tensor arranged as $|V_{zz}| > |V_{yy}| > |V_{xx}|$. The quadrupole moments Q were taken as 19.60×10^{-30} m^2 for ^{73}Ge and 2.56×10^{-30} m^2 for ^{17}O [29]. Typical solid-state NMR experiments access only the magnitude of $C_{\rm Q}$, therefore we present the absolute values, $|C_{\rm Q}|$ and obtain mean values of $|C_{\rm Q}|$. However, to aid the discussion in figure 2 we plot $C_{\rm Q}$ to demonstrate the sign variation.

3. Results and discussion

Isotropic chemical shieldings and quadrupole coupling constants were calculated for all atoms in the two models of vitreous GeO_2, as well as for quartz GeO_2. The average values for ^{73}Ge and ^{17}O are summarized in tables 1 and 2, respectively.

Table 1. Calculated mean values of ^{73}Ge isotropic chemical shift (δ_{iso}), quadrupole coupling constant (C_Q) and asymmetry parameter (η) for models A and B of vitreous GeO_2, quartz GeO_2, and available experimental data. Values in the brackets indicate the standard deviation from the mean value.

	δ_{iso} (ppm)	C_Q (MHz)	η
Model A	−152 (28)	17.7 (8.8)	0.52 (0.26)
Model B	−127 (11)	18.6 (3.6)	0.54 (0.22)
Quartz	−110	8.10	0.70
Expt[a] quartz	−110	9.2	0.5
Expt[a] v-GeO_2	−30	<10.5	
Expt[b] v-GeO_2	50 to −100	8–10	

[a] Reference [26]. [b] Reference [30].

Table 2. Calculated mean values of ^{17}O isotropic chemical shift (δ_{iso}), quadrupole coupling constant (C_Q) and asymmetry parameter (η) for models A and B of vitreous GeO_2, quartz GeO_2, and available experimental data. Values in the brackets indicate the standard deviation from the mean value.

	δ_{iso} (ppm)	C_Q (MHz)	η
Model A	92 (19)	8.6 (0.93)	0.51 (0.21)
Model B	85 (16)	7.95 (0.58)	0.66 (0.23)
Quartz	50	7.59	0.57
Expt[a] quartz	50	7.05	0.53
Expt[b] quartz	70	7.3	0.48
Expt[a] v-GeO_2	42	7.4	0.53
Expt[b] v-GeO_2	70	7.1	0.48

[a] Reference [27]. [b] Reference [31].

We first explored correlations between the chemical shifts of ^{73}Ge and ^{17}O and the Ge–O–Ge angles. Both models of vitreous GeO_2 represent a good range of Ge–O–Ge angles with, for example, the angles in model A ranging from 110° to 170°. For the shifts of ^{73}Ge, we searched for a correlation with the average of the four neighboring Ge–O–Ge bond angles. Such a correlation was first suggested experimentally for silica polymorphs and zeolites [32, 33], and later confirmed by first-principles calculations for various oxide systems [15, 13]. In figure 1(a), the isotropic shifts δ_{iso} of ^{73}Ge are plotted against the average of the four nearby Ge–O–Ge angles, revealing a clear linear correlation. Recent experimental results [26] report the mean ^{73}Ge isotropic shift of vitreous GeO_2 at −30 ppm. This value is noticeably different than our calculated results for model A (152 ppm) and model B (127 ppm). The authors of [26] admit some experimental uncertainty, in particular we note their value is dependent on their estimate of C_Q. However, the origin of the large size of this discrepancy remains unclear at present. Consequently, we are unable to use this experimental result to extract useful structural information, as has been done previously for other glasses [15, 13].

In figure 1(b), we plot ^{17}O δ_{iso} against the local angle Ge–O–Ge. The calculated results reveal a clear trend with increasing angle, highlighting the sensitivity of ^{17}O NMR as a structural probe. However, the scattering is significant, suggesting that the shielding is also affected by structural variation beyond the length scale of nearest-neighbor atoms. A similar behavior has previously been found for silicates and zeolites [14].

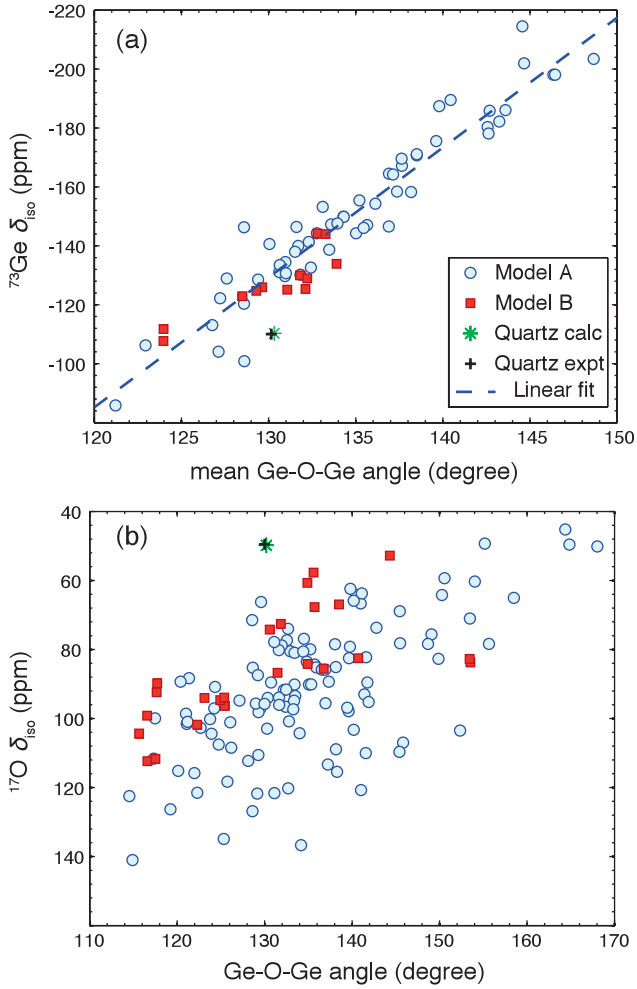

Figure 1. (a) Calculated ^{73}Ge NMR isotropic shifts versus the mean Ge–O–Ge angle associated with the considered Ge atom (for each Ge, the average is over four Ge–O–Ge angles) and (b) calculated ^{17}O NMR isotropic shifts versus the local Ge–O–Ge angle. Blue circles represent results from model A and dark red squares those from model B. The green star represents the calculated result for quartz GeO_2 and the black cross the ^{73}Ge experimental results of [26] and the ^{17}O experimental result of [27]. For quartz GeO_2 all the four Ge–O–Ge angles are the same and equal to 130.2°. The blue dashed line corresponds to a linear regression of the data.

We then explored correlations between the EFG parameters of both ^{73}Ge and ^{17}O and underlying structural features. For ^{73}Ge, we were unable to find a correlation with any trivial local structural property (not shown), more specifically no correlation was found for C_Q with the change in bond length nor with the deviation in O–Ge–O angles from the ideal tetrahedral angle. Furthermore, the average calculated values of ^{73}Ge C_Q for our vitreous models A (17.7 MHz) and B (18.6 MHz) are much higher than both the recent experimental value of 10.5 MHz [26] and the range of 8–10 MHz suggested by earlier experimental data [30]. In figure 2, we plot the distribution of C_Q values for models A and B. The range of $|C_Q|$ values calculated in model A varies from 8 to 40 MHz. The sign of the quadrupole coupling constant is clearly biased towards the negative region. For comparison, we also plot the calculated and experimental results for quartz GeO_2 which are

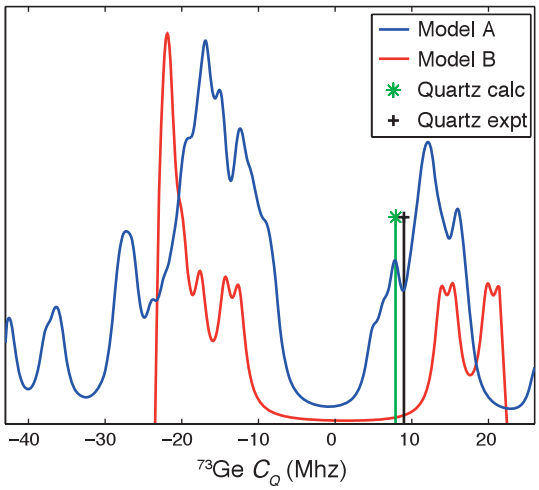

Figure 2. Distribution of calculated quadrupole coupling constants C_Q for ^{73}Ge in vitreous GeO_2. The blue line represent results from model A and the dark red line those from model B. The green star represents the calculated result for quartz GeO_2 and the black cross the ^{73}Ge experimental results of [26].

in good agreement. It should be noted that the electric field gradient at Ge sites in vitreous GeO_2 is typically an order of magnitude smaller than at O sites. This is expected due to the tetrahedral coordination of Ge. The sizable values of C_Q for ^{73}Ge instead arise from its large nuclear quadrupole moment.

Our investigation of the ^{17}O EFG parameters was more successful. In figure 3, we plot C_Q and η for ^{17}O against the local angle Ge–O–Ge. The ^{17}O quadrupole coupling constant C_Q shows a linear correlation with the Ge–O–Ge bond angle, providing further support to the relationship which was previously suggested on the basis of cluster calculations for quartz GeO_2 [34, 35]. For the asymmetry parameter η, we also find a clear correlation, showing a characteristic dependence which has also been observed for quartz GeO_2 [34, 35] and crystalline SiO_2 systems [14]. Similar trends were also observed for calcium aluminosilicate [16] and sodium tetrasilicate [17] glasses.

In order to extract information concerning the Ge–O–Ge bond angle distribution of vitreous GeO_2, we use ^{17}O quadrupole coupling constants C_Q experimentally determined for GeO_2 glasses [31, 27]. We proceed by fitting a linear correlation to the combined results of models A and B in figure 3(a). A linear relation was found to give a higher correlation coefficient than the cosine function used for other glasses [16, 17]. However, the correlation obtained in this way cannot be used directly to relate the measured C_Q values to the Ge–O–Ge angles, because of the intrinsic error of density functional calculations and finite size effects preventing optimal structural relaxation in our models. Therefore, we calibrated the correlation by considering quartz GeO_2 for which no structural ambiguity subsists. We impose that the relationship associates the experimentally determined value of $C_Q = 7.05$ MHz [27] with the angle of 130° corresponding to this structure. Thus, the finally adopted correlation is obtained by a rigid downwards shift which preserves the slope derived

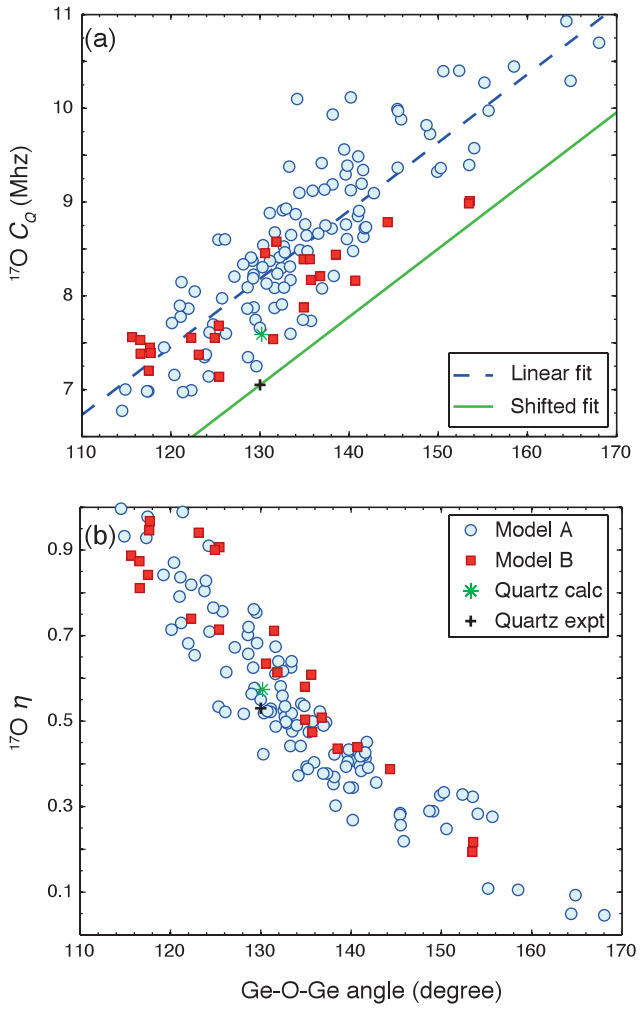

Figure 3. Calculated (a) quadrupole coupling constant C_Q and (b) asymmetry parameter η for ^{17}O in vitreous GeO_2 NMR versus the local Ge–O–Ge angle. In (a), the blue dashed line is obtained by a linear regression of the calculated results. The green solid line is calibrated to the experimental result for quartz GeO_2 but preserves the slope derived from the first-principles results. Other symbols as in figure 1.

from our first-principles study (figure 3), and is given by

$$C_Q\ (\text{MHz}) = 0.0727\theta\ (\text{deg}) - 2.395. \qquad (5)$$

The bond angles derived through this relation from two sets of experimental C_Q are given in table 3. Focusing on the most recent experimental data [27], we derive a Ge–O–Ge angle of 135° from the mean C_Q value of 7.4 MHz. Experimental values for C_Q range from 6.6 to 7.7 MHz [27], corresponding to angles of 124° and 139°, respectively. The mean value and the range of angles determined in the present study are in agreement with those inferred from both diffraction [5, 8] and Raman [10, 11] experiments.

4. Conclusion

NMR parameters of ^{73}Ge and ^{17}O in vitreous GeO_2 and quartz GeO_2 were determined through density functional

Table 3. Average Ge–O–Ge angle in vitreous GeO_2 derived from experimental measurements of quadrupole coupling constants C_Q through equation (5).

	∠Ge–O–Ge	
C_Q (MHz)	Previous	Present
7.4[a]		135°
7.1[b]	130°[b]	131°

[a] Reference [27].
[b] Reference [31].

calculations and correlated with local structural features. A linear correlation was observed between the ^{73}Ge isotropic shift and the mean of the four neighboring Ge–O–Ge bond angles, in accordance with a general trend observed for oxides. For ^{17}O, clear correlations were observed for C_Q and η as a function of the Ge–O–Ge bond angle. In combination with available experimental data for C_Q in vitreous GeO_2 [27], the derived correlation allowed us to extract a mean Ge–O–Ge bond angle of 135° and to determine the range of such angles in the glass (124°–139°). The achieved description further corroborates the picture inferred from diffraction [5, 8] and Raman [10, 11] measurements.

Acknowledgments

We thank P S Salmon and M E Smith for their suggestions and L Giacomazzi for providing us with the models of vitreous GeO_2. We also acknowledge fruitful interactions with P Broqvist. Computing resources were provided by the Cambridge High Performance Computing Service HPCS and were funded by EPSRC Grant EP/F0327731/1.

References

[1] Polukhin V N 1982 *Sov. J. Glass Phys. Chem.* **8** 249–53
[2] Margaryan A and Piliavin M 1993 *Prospects of Using Germanium-Dioxide-Based Glasses for Optics* (London: Artech House Publishers)
[3] Margaryan A and Liu W M 1993 *Opt. Eng.* **32** 1995–6
[4] Houssa M, Satta A, Simoen E, De Jaeger B, Caymax M, Meuris M and Heyns M 2007 *Germanium Based Technologies: From Materials to Devices* (Amsterdam: Elsevier)
[5] Neuefeind J and Liss K 1996 *Ber. Bunsenges. Phys. Chem.* **100** 1341–9
[6] Sampath S, Benmore C J, Lantzky K M, Neuefeind J, Leinenweber K, Price D L and Yarger J L 2003 *Phys. Rev. Lett.* **90** 115502
[7] Salmon P S, Barnes A C, Martin R A and Cuello G J 2006 *Phys. Rev. Lett.* **96** 235502
[8] Salmon P S, Barnes A C, Martin R A and Cuello G J 2007 *J. Phys.: Condens. Matter* **19** 415110
[9] Umari P, Gonze X and Pasquarello A 2003 *Phys. Rev. Lett.* **90** 027401
[10] Giacomazzi L, Umari P and Pasquarello A 2005 *Phys. Rev. Lett.* **95** 075505
[11] Giacomazzi L, Umari P and Pasquarello A 2006 *Phys. Rev.* B **74** 155208
[12] Giacomazzi L, Umari P and Pasquarello A 2009 *Phys. Rev.* B **79** 064202
[13] Umari P and Pasquarello A 2005 *Phys. Rev. Lett.* **95** 137401
[14] Profeta M, Mauri F and Pickard C J 2003 *J. Am. Chem. Soc.* **125** 541–8
[15] Mauri F, Pasquarello A, Pfrommer B G, Yoon Y G and Louie S G 2000 *Phys. Rev.* B **62** R4786
[16] Benoit M, Profeta M, Mauri F, Pickard C J and Tuckerman M E 2005 *J. Phys. Chem.* B **109** 6052–60
[17] Charpentier T, Ispas S, Profeta M, Mauri F and Pickard C J 2004 *J. Phys. Chem.* B **108** 4147–61
[18] Haines J, Cambon O, Philippot E, Chapon L and Hull S 2002 *J. Solid State Chem.* **166** 434–41
[19] Fletcher D, McMeeking R and Parkin D 1996 *J. Chem. Inf. Comput. Sci.* **36** 746–9
[20] Pickard C J and Mauri F 2001 *Phys. Rev.* B **63** 245101
[21] Clark S J, Segall M D, Pickard C J, Hasnip P J, Probert M J, Refson K and Payne M C 2005 *Z. Kristallogr.* **220** 567–70
[22] Yates J R, Pickard C J and Mauri F 2007 *Phys. Rev.* B **76** 024401
[23] Vanderbilt D 1990 *Phys. Rev.* B **41** 7892–5
[24] Perdew J P, Burke K and Ernzerhof M 1996 *Phys. Rev. Lett.* **77** 3865–8
[25] Monkhorst H J and Pack J D 1976 *Phys. Rev.* B **13** 5188
[26] Michaelis V K, Aguiar P M, Terskikh V V and Kroeker S 2009 *Chem. Commun.* 4660–2
[27] Du L S and Stebbins J F 2006 *J. Phys. Chem.* B **110** 12427–37
[28] Petrilli H M, Blöchl P E, Blaha P and Schwarz K 1998 *Phys. Rev.* B **57** 14690
[29] Pyykkö P 2001 *Mol. Phys.* **99** 1617–29
[30] Stebbins J F, Du L S, Kroeker S, Neuhoff P, Rice D, Frye J and Jakobsen H J 2002 *Solid State Nucl. Magn. Reson.* **21** 105–15
[31] Hussin R, Dupree R and Holland D 1999 *J. Non-Cryst. Solids* **246** 159–68
[32] Smith J V and Blackwell C S 1983 *Nature* **303** 223–5
[33] Ramdas S and Klinowski J 1984 *Nature* **308** 521–3
[34] Clark T M and Grandinetti P J 2000 *J. Non-Cryst. Solids* **265** 75–82
[35] Sefzik T H, Clark T M and Grandinetti P J 2007 *Solid State Nucl. Magn. Reson.* **32** 16–23